Journal of Environmental Management 309 (2022) 114669

Contents lists available at ScienceDirect

Journal of Environmental Management

journal homepage: www.elsevier.com/locate/jenvman

Removal of microcystin (MC-LR) in constructed wetlands integrated with microbial fuel cells: Efficiency, bioelectricity generation and microbial response

Rui Cheng [a,b], Hui Zhu [a,b,*], Jingfu Wang [c], Shengnan Hou [a,b], Brian Shutes [d], Baixing Yan [a,b]

[a] Key Laboratory of Wetland Ecology and Environment, Northeast Institute of Geography and Agroecology, Chinese Academy of Sciences, Changchun, 130102, China
[b] Jilin Provincial Engineering Center of CWs Design in Cold Region and Beautiful Country Construction, Changchun, 130102, China
[c] State Key Laboratory of Environmental Geochemistry, Institute of Geochemistry, Chinese Academy of Sciences, Guiyang, 550081, China
[d] Department of Natural Sciences, Middlesex University, Hendon, London, NW4 4BT, UK

ARTICLE INFO

Keywords:
Constructed wetlands
Microbial fuel cells
Eutrophication
Microcystins
Microbial community

ABSTRACT

Microcystins (MCs) pollution caused by cyanobacteria harmful blooms (CHBs) has posed short- and long-term risks to aquatic ecosystems and public health. Constructed wetlands (CWs) have been verified as an effective technology for eutrophication but the removal performance for MCs did not achieve an acceptable level. CWs integrated with microbial fuel cell (MFC-CWs) were developed to intensify the nutrient and Microcystin-LR (MC-LR) removal efficiencies in this study. The results indicated that closed-circuit MFC-CWs (T1) exhibited a better NO_3^--N, NH_4^+-N, TP and MC-LR removal efficiency compared to that of open-circuit MFC-CWs (CK, i.e., traditional CWs). Therein, a MC-LR removal efficiency of greater than 95% was observed in both trials in T1. The addition of sponge iron to the anode layer of MFC-CWs (T2) improved only the NO_3^--N removal and efficiency bioelectricity generation performance compared to T1, and the average effluent MC-LR concentration of T2 (1.14 μg/L) was still higher than the provisional limit concentration (1.0 μg/L). The microbial community diversity of T1 and T2 was simplified compared to CK. The relative abundance of *Sphingomonadaceae* possessing the degradation capability for MCs increased in T1, which contributed to the higher MC-LR removal efficiency compared to CK and T2. While the relative abundance of electrochemically active bacteria (EAB) (i.e., *Desulfuromonadaceae* and *Desulfomicrobiaceae*) in the anode of T2 was promoted by the addition of sponge iron. Overall, this study suggests that integrating MFC into CWs provides a feasible intensification strategy for eutrophication and MCs pollution control.

1. Introduction

Cyanobacteria harmful blooms (CHBs) induced by eutrophication and climate change have become a serious problem worldwide (Conley et al., 2009). Beside the undesirable taste and odor during CHBs, some of cyanobacteria can produce various cyanotoxins to maintain ecological dominance of cyanobacteria in aquatic environments (Liu et al., 2020). Microcystins (MCs), with hepatotoxic and tumor promoting activities, are considered to be one of the most persistent and hazardous groups among extensive cyanotoxins (Lin et al., 2016). In the last few decades, MCs have been detected in freshwater and food webs worldwide (Kim et al., 2021; Machado et al., 2017). Therefore, MCs in water and food were verified to cause various adverse health events globally and pose health risks to human beings and animals (Pham and Utsumi, 2018; Wang et al., 2021). The World Health Organization (WHO) has set a provisional drinking water guideline value of 1.0 μg/L for MC-LR as the highest acceptable microcystin equivalents concentration (World Health Organization, 2017).

Some treatment technologies, including physical, chemical and advanced oxidation processes, have already been applied to reduce the potential risk of MCs pollution (Dixit et al., 2019). However, the above treatment technologies are limited by their high cost and/or low efficiency, the harmful by-products and MC derivatives generated. In addition, some treatment technologies require the development of sophisticated techniques when they are used on a large-scale (Tsao et al., 2017). Therefore, more environment-friendly and economical

* Corresponding author. Key Laboratory of Wetland Ecology and Environment, Northeast Institute of Geography and Agroecology, Chinese Academy of Sciences, Changchun, 130102, China.
E-mail address: zhuhui@iga.ac.cn (H. Zhu).

https://doi.org/10.1016/j.jenvman.2022.114669
Received 13 September 2021; Received in revised form 11 January 2022; Accepted 2 February 2022
Available online 12 February 2022

technologies urgently need to be developed to control eutrophication and MCs pollution. CWs have been widely recognized as green technology for treating wastewater originating from municipal engineering, industry and agriculture since 1950s due to their lower operating cost, environmental benefits and less maintenance requirements (Zhu et al., 2011; Yu et al., 2019; Liang et al., 2018; Chen et al., 2020). Therefore, we infer that CWs may be a promising method for treating eutrophic water containing MCs, which could resolve eutrophication and MCs pollution from its source.

According to our previous study, the potential risk of MCs still existed due to due to the stable cyclic structure of MCs (Cheng et al., 2021). Therefore, how to degrade MCs rapidly and completely in CWs needs to be further explored. In recent years, various treatment technologies were coupled with traditional CWs, which was shown to maximize their combined advantages (Lutterbeck et al., 2020; Wang et al., 2020). As an emerging wastewater treatment technology, microbial fuel cells (MFC) have aroused increasing interest worldwide (Prathiba et al., 2022; Wang et al., 2020). More than 90% of MCs can be degraded in MFC, because MFC provides a more favorable electron pathway for the decomposition of MCs (Yuan et al., 2011). However, the application of MFC in scale-up operations is challenging due to high cost and complex operation and maintenance. CWs integrated with microbial fuel cell (MFC-CWs) can overcome some limitations of both technologies (Doherty et al., 2015). As an advanced wastewater treatment technology, MFC-CWs have exhibited the capacity for promoting various contaminants removal, including heavy metals, inorganic non-metals, and refractory organics (Wang et al., 2019a; Wen et al., 2020; Wen et al., 2021b). Although MFC-CWs show higher removal efficiency in treating various wastewater, there are still some practical limitations that should be overcome, for example, lower refractory organics removal efficiency, unsatisfactory power output and high internal resistance (Xu et al., 2019).

To date, very limited research is available on MCs removal in MFC-CWs. The effectiveness and mechanism of detailed MCs degradation through biological approaches in MFC-CWs remains unknown. The feasibility of directly producing bioelectricity from eutrophic water containing MCs in MFC-CWs has not yet been reported. The addition of zero valent iron (ZVI) into the anode of MFC has been reported to promote the degradation of some refractory organics (e.g., PAHs and antibiotics, etc) and generation of bioelectricity due to the role of ZVI as an electron donor (Wang et al., 2019a). Whether the addition of ZVI can improve MC-LR removal efficiency and bioelectricity generation also needs to be identified.

In this study, MC-LR was selected as a model to represent MCs. MFC-CWs with open-circuit were set up as control treatment (i.e., traditional CWs). Closed circuit MFC-CWs and MFC-CWs with the addition of sponge iron into the anode were used to investigate the performance of eutrophication control and MCs pollution treatment as well as bioelectricity generation performance. The main objectives are to (1) evaluate the removal capacity of a typical MCs variant (i.e., MC-LR) and nutrients from eutrophic water in MFC-CWs; (2) reveal the nutrients and MCs removal mechanism in MFC-CWs; (3) investigate how sponge iron affects electricity generation and MCs degradation. This study can provide both a theoretical and practical basis for MFC-CWs applied in eutrophication and MCs pollution control.

2. Materials and methods

2.1. The design and construction of MFC-CWs

A group of microcosm-scale MFC-CWs were constructed at Northeast Institute of Geography and Agroecology, Chinese Academy of Sciences (CAS), Changchun, China. The schematic diagram of the MFC-CW reactors (height 49 cm; internal diameter 20 cm; material polyethylene plastic) is shown in Fig. 1a. Each MFC-CW was filled with a 15 cm of quartz (diameter of 6–7 mm) layer, a 10 cm of anode layer, a 15 cm of quartz middle layer, and a 5 cm of cathode layer respectively from bottom to top. Three treatments established in this study were open-circuit MFC-CWs (CK), closed-circuit MFC-CWs (T1) and closed-circuit MFC-CWs with the addition of sponge iron into anode (T2), respectively. There were three replicates for each treatment. The cathode and anode of all reactors were filled with granular activated carbon (GAC) that was pretreated by mixing with fresh sludge. Stainless-steel mesh was buried in the middle of GAC layer of T1 and T2 to collect the electrons. While the anode of T2 was filled with the mixture of activated carbon and sponge iron (a type of low-cost material with main

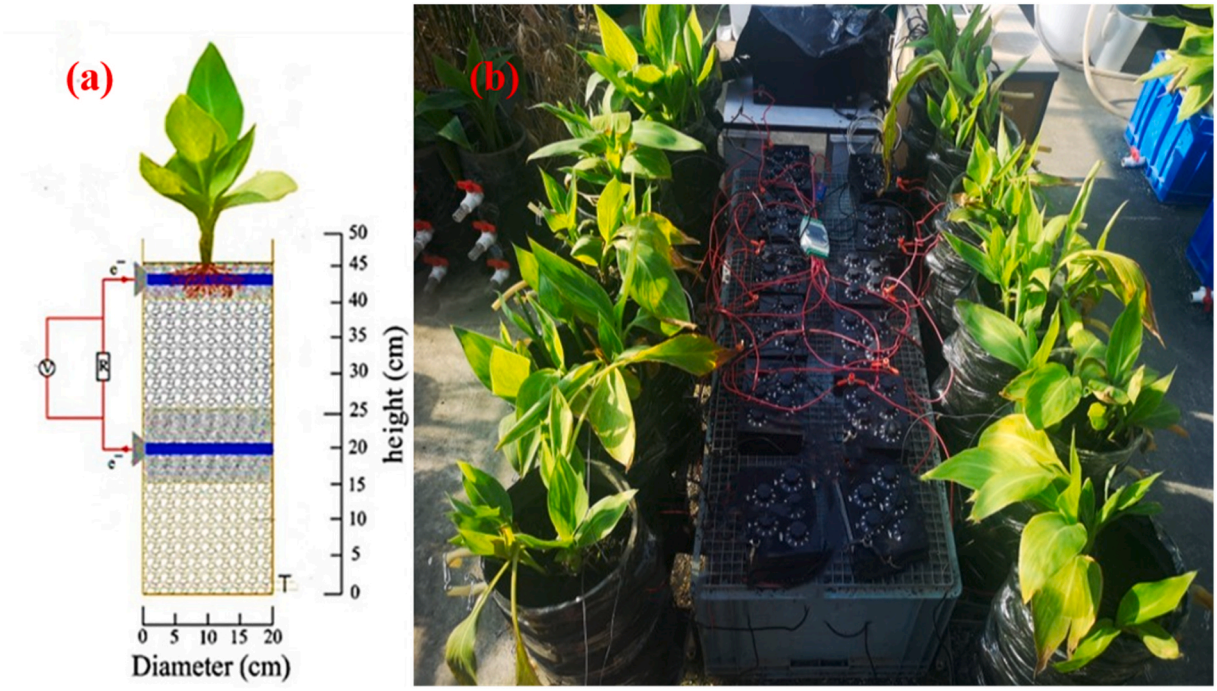

Fig. 1. Schematic diagram (a) and a photo(b) of the MFC-CWs.

component ZVI). The specific surface areas and pore sizes of anode of T1 and T2 are presented in Table 1. Mature *Canna indica* were planted in the cathode layer of each MFC-CWs with an initial density of 3 plants per reactor. Before the formal experiment, all the MFC-CWs have been operating stably for five months for domestic wastewater treatment. Closed-circuit MFC-CWs were connected with an external adjustable resistance of 1000 Ω.

MC-LR used for preparing the influent was extracted and purified from algal cultures of *Microcystis aeruginosa* FACHB-905 (purchased from Freshwater Algae Culture, Institute of Hydrobiology, Chinese Academy of Sciences). The extracted and purified procedures followed the methods demonstrated by Morón-López et al. (2019). MC-LR standard used in quantitative analysis was obtained from Taiwan Algal Science, Inc, China. Before analysis, MC-LR standard was dissolved in methanol and stored at −20 °C as stock solution prepared with a concentration of 100 μg/mL. High Performance Liquid Chromatography (HPLC)-grade methanol and trifluoroacetic acid (TFA) were used to prepare HPLC mobile phase. All the other chemicals applied in this study were of reagent grade.

2.2. Experimental design and operation

The reported maximum MCs concentration in freshwater of China was 16.84 μg/L, which was observed in Taihu Lake (Shi et al., 2015). Therefore, the influent MC-LR concentration in this study was designed as 15 μg/L. The concentrations of other contaminants in the synthetic wastewater were as follows: NH_4^+-N (2.5 mg/L), NO_3^--N (3.5 mg/L), and TP (1 mg/L), which was prepared by NH_4Cl, KNO_3, and KH_2PO_3. Each operation trial of the batch experiment was 2 days. During the operation period, 5 L wastewater was added to the top of the reactors.

2.3. Sampling and analytical methods

The effluent samples were collected per 12 h to evaluate the nutrient removal efficiency. By the end of each batch, a total of 1 L water samples was collected from the drainage tap of each MFC-CW for quantifying the MC-LR removal efficiency. The NH_4^+-N, NO_3^--N and TP concentrations were measured by automatic chemical analyzer (Smartchem 200, Italy). Before measurement, all the samples were filtered through 0.45 μm filters. MC-LR concentration was determined by (HPLC) with UV detector (Waters 2695e). The collection, preparation and methods of analysis have been recorded in our previous study (Cheng et al., 2021), which is also available in the complementary document (Text S1).

The substrate samples were collected from each layer of the MFC-CWs in centrifuge tubes at the end of the entire experiment following the methods described by Chen et al. (2020). All samples were sent to Sangon Biotech Co., Ltd. (China) for analysis. Illumina high-throughput sequencing was conducted to analyze the microbial community diversity and structure of each sample. RDP (Ribosomal Database Project) database (http://rdp.cme.msu.edu/index.jsp) was selected as the database used in analysis.

2.4. Bioelectricity generation and electrochemical analysis

The voltage output across the external resistance during the entire operation cycles was monitored and recorded per 0.5 h by a data acquisition module (DAM-3057, ART Technology Co. Ltd., China). The power density curve and polarization curve were plotted according to published methods (Lu et al., 2015).

Table 1
Specific surface areas and pore sizes of two kinds of anode (T1: closed-circuit MFC-CWs; T2: closed-circuit MFC-CWs amended with sponge iron in anode).

	Surface area (m^2/g)	Total pore volume (mL/g)	Micropore volume (mL/g)	Pore diameter (nm)
T1	172.569	0.104	0.059	3.827
T2	21.372	0.014	0.006	5.587

2.5. Statistical analysis

Statistical analyses were performed using the SPSS 19.0 (SPSS Inc., Chicago, USA). All the data in this study were presented as mean ± SD. Means between different treatments were compared by one-way analysis of variance (One-way ANOVA) with Tukey HSD test at the significance level of 0.05. All figures were designed and plotted by Origin 8.5 (Origin Lab Inc., USA).

3. Results

3.1. Nutrient removal in MFC-CWs

The effluent NH_4^+-N concentration of all the treatments decreased with increasing operation time during the two operation cycles (Fig. 2a). The average final effluent NH_4^+-N concentration of three treatments was 0.403 mg/L (CK), 0.251 mg/L (T1) and 0.306 mg/L (T2), respectively, which all met Class II of the Environmental Quality Standard for Surface Water (GB3838-2002) in China. The average removal efficiency of CK, T1 and T2 was 84.95%, 90.62% and 88.56%, respectively. The average NH_4^+-N removal efficiency of CK during the entire operation cycles was significantly ($p < 0.05$) lower than other treatments. At 12 h, the removal efficiency of T1 was significantly ($p < 0.05$) higher than other treatments.

All treatments exhibited good NO_3^--N removal efficiency during the entire experiment and in Trial 2, the final NO_3^--N removal efficiency of all treatments was up to 100% (Fig. 2b). During the entire experiment, the effluent NO_3^--N concentration of T1 (0.067 mg/L) and T2 (0 mg/L) at 12 h was significantly ($p < 0.05$) lower than that of CK (0.208 mg/L). The best NO_3^--N removal performance throughout the entire experiment was observed in T2. The NO_3^--N of T2 was completely removed in the first 12 h in Trial 2.

TP removal efficiency of three treatments is presented in Fig. 2c. Compared to the influent TP concentration, the significant ($p < 0.05$) decrease in TP effluent concentrations of all treatments mainly occurred in the first 12 h. The effluent TP concentration of all treatments changed slightly in the remaining operation time. The average final TP effluent concentrations of three treatments were 0.558 mg/L (CK), 0.201 mg/L (T1) and 0.461 mg/L (T2), respectively. The average removal efficiency of T1 throughout the entire experiment was significantly ($p < 0.05$) better than other treatments.

3.2. MC-LR removal

The average MC-LR removal efficiency of all treatments in both Trials 1 and 2 exceeded 90% (Fig. 3) and was significantly ($p < 0.05$) higher in T1 with the average removal percentage of 97.19% and 95.21% for Trial 1 and 2, respectively. The lowest removal efficiency was observed in T2, which showed a significant ($p < 0.05$) difference with that of CK and T1. The effluent MC-LR concentration of CK and T1 did not exceed the WHO provisional limit concentration (1 μg/L) but the average effluent MC-LR concentration of T2 was 1.14 μg/L.

3.3. Bioelectricity generation

Power density and polarization curves of two types of closed-circuit MFC-CWs (T1 and T2) during the stable operation phase are presented in Fig. 4a. The average maximum power density of T1 and T2 was 8.67 mW m^{-3} and 35.84 mW m^{-3}, respectively. The corresponding current density of T1 and T2 was 114.70 mA m^{-2} and 573.48 mA m^{-2}. Polarization curves were plotted by adjusting a variable resistor with a range of 50–100,000 Ω and were performed to gain an understanding of the internal resistance in closed circuit MFC-CWs. According to Ohm's law,

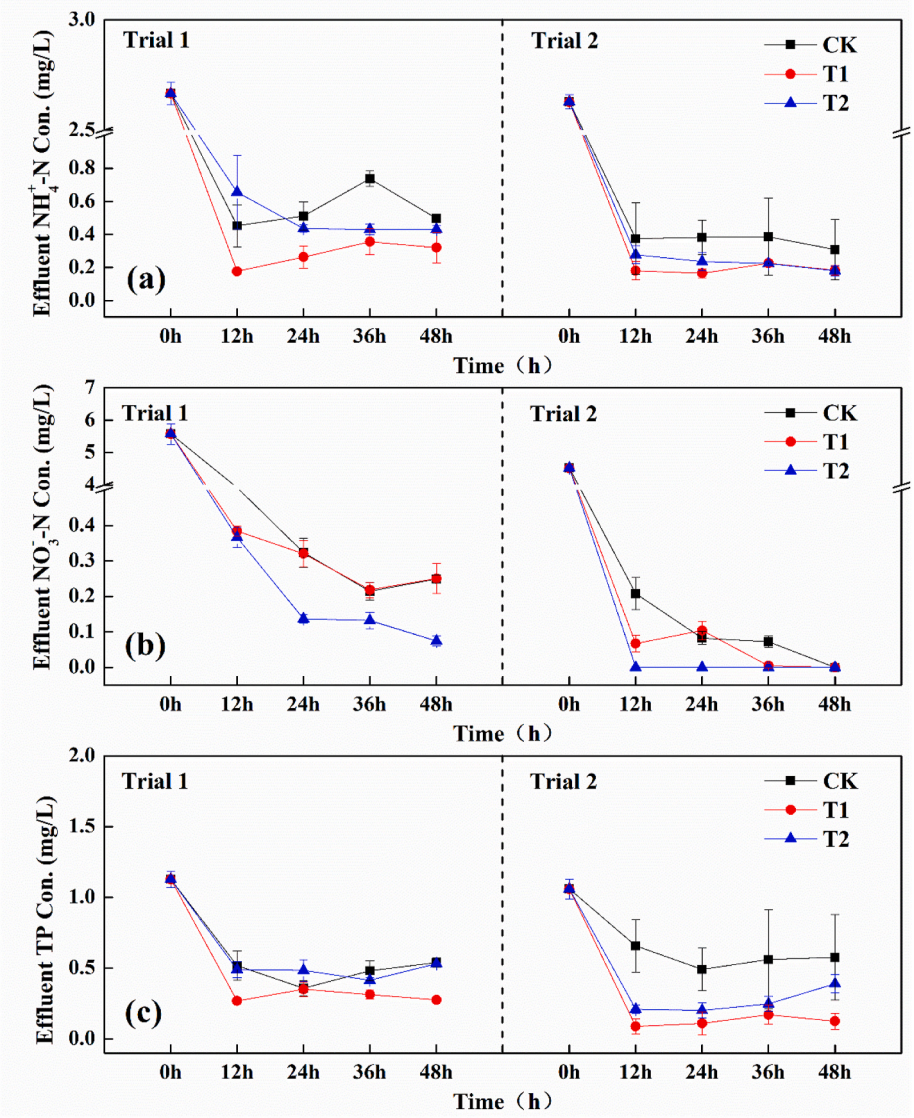

Fig. 2. Effluent NH_4^+-N (a), NO_3^--N (b) and TP (c) concentrations in three types of MFC-CWs. (CK: open-circuit MFC-CWs; T1: closed-circuit MFC-CWs; T2: closed-circuit MFC-CWs amended with sponge iron in anode). Values represent the mean of three replicates and error bars represent the standard deviation.

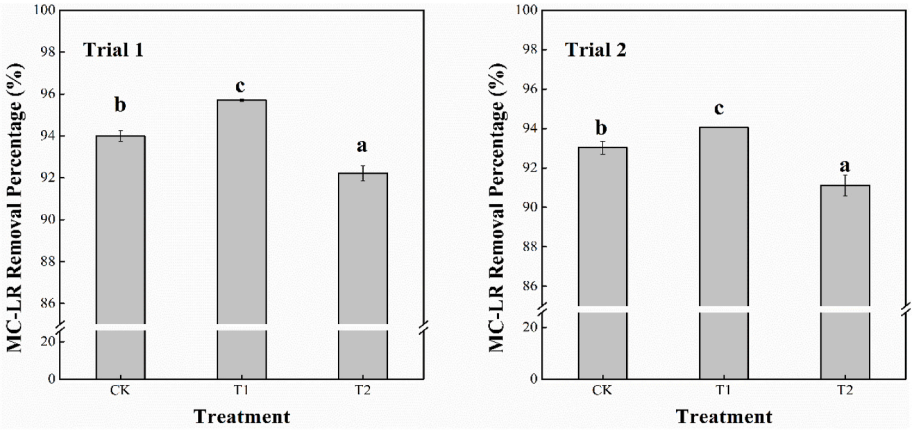

Fig. 3. MC-LR removal percentage in MFC-CWs (CK: open-circuit MFC-CWs; T1: closed-circuit MFC-CWs; T2: closed-circuit MFC-CWs amended with sponge iron in anode). Values represent the mean of three replicates and error bars represent the standard deviation.

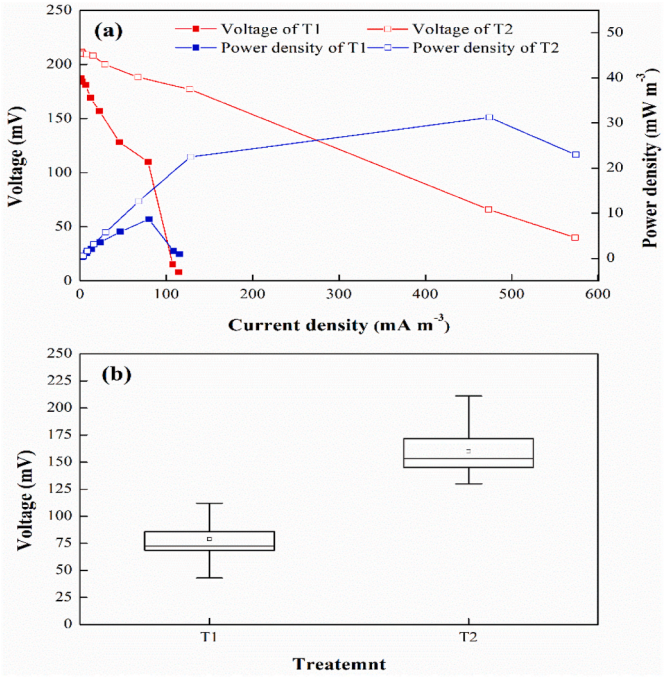

Fig. 4. The bioelectricity generation performance of two type of closed-circuit MFC-CWs. (a) polarization and power density curves, (b) bioelectricity generation. (T1: closed-circuit MFC-CWs; T2: closed-circuit MFC-CWs closed-circuit MFC-CWs amended with sponge iron in anode).

the internal resistance of T2 was 217.18 Ω, which was much lower than that of T1 (1138.8 Ω). The voltage of T1 and T2 is illustrated in Fig. 4b. The average voltage of T1 and T2 during the operation time was 78.88 ± 15.12 mV and 159.89 ± 19.18 mV, respectively. The voltage of T2 was significantly ($p < 0.05$) higher than that of T1.

3.4. Microbial community analysis of anode and cathode layers of three types of MFC-CWs

3.4.1. The richness and diversity of microbial community

The microbial community richness and diversity in the anode and cathode of different treatments are presented in Table 2. The operational taxonomic units (OTUs) number of three types of MFC-CWs was ranged from 1243 to 2070. The Goods Coverage in all treatments was higher than 0.98, which indicated that most of the species in each type of reactor were detected. The Chao index was used to evaluate the richness of the microbial community, which were in the order of CK-Anode (2631) > CK-Cathode (2621) > T1-Cathode (1965) > T1-Anode (1655) > T2-Cathode (1826) > T2-Anode (1243). A similar trend was observed with the Shannon index, which reflected the diversity of the microbial community. The values of the Shannon index in T2 were 4.13 (anode) and 5.59 (cathode), respectively, which were lower than those in CK (5.60 in anode and 5.88 in cathode) and T1 (4.63in anode and 5.86 in cathode). Under open-circuit operation mode, i.e., CK treatment, there was no significant difference in the values of the OTUs number and Shannon and Chao index between anode and cathode. The closed-circuit operation (i.e., T1 and T2) reduced the richness and diversity of the microbial community. However, the values of the above indexes for the anode were lower than those for the cathode in the two types of closed-circuit MFC-CWs. The use of sponge iron (T2) decreased the microbial richness and diversity of microbial community compared to that of T1.

Table 2
Summary statistics of microbial community diversity indices in MFC-CWs.

	OTUs	Shannon	Chao	Coverage
CK-Anode	2068 ± 158	5.60 ± 0.33	2630.59 ± 122.18	0.98 ± 0.002
CK-Cathode	2070 ± 57	5.88 ± 0.15	2621.10 ± 31.44	0.98 ± 0.001
T1-Anode	1655 ± 101	4.63 ± 0.74	2287.47 ± 48.62	0.98 ± 0.001
T1-Cathode	1965 ± 176	5.86 ± 0.10	2472.09 ± 173.59	0.99 ± 0.001
T2-Anode	1243 ± 113	4.13 ± 0.35	1868.49 ± 177.98	0.99 ± 0.001
T2-Cathode	1826 ± 11	5.59 ± 0.38	2382.75 ± 52.46	0.98 ± 0.001

3.4.2. The microbial community composition

The microbial community composition of each treatment at phylum, order and family level is presented in Fig. 5. At phylum level (Fig. 5a), *Proteobacteria* (29.30–52.8%) was the most predominant phylum in the anode of all treatments, followed by *Firmicutes* (8.0–22.1%), *Actinobacteria* (7.9–13.4%), *Chloroflexi* (3.4–13.1%) and *Planctomycetes* (1.4–9.4%). The highest relative abundance of *Proteobacteria* and *Firmicutes* was observed in T2 (52.8%) and T1 (22.1%), respectively. The microbial community composition in the cathode of the three treatments at phylum level was similar, and *Proteobacteria* (40.0–43.1%), *Actinobacteria* (7.6–10.6%), *Planctomycetes* (9.4–10.8%) constitute the key phyla in the cathode of all MFC-CWs.

As presented in Fig. 5b, *Rhodocyclales* (10.8–12.2%), *Anaerolineales* (3.0–10.6%), *Pseudomonadales* (2.1–14.8%), *Rhizobiales* (4.2–5.1%), *Planctomycetales*, (1.4–9.8%) and *Actinomycetales* (0.9–6.7%) were the dominant order in the anode of the three treatments. Besides these predominant orders, the relative abundance of *Burkholderiales* (0.9–11.4%), *Sphingomonadales* (0.3–1.2%) and *Xanthomonadales* (0.9–4.6%) in the anodic community was higher than that of other microorganisms. The relative abundance of *Desulfuromonadales* (4.4%) and *Desulfovibrionales* (2.6%) of T2 was higher than in the other treatments. The relative abundance of the above microorganisms was promoted by the addition of sponge iron. The community in the cathode of all MFC-CWs mainly consisted of *Rhizobiales* (15.4–17.9%), *Planctomycetales* (9.1–10.5%), *Rhodocyclales* (3.6–8.8%) and *Actinomycetales* (5.8–8.4%). Furthermore, the higher relative abundance of *Rhodospirillales* (2.5–3.0%), *Rhodobacterales* (1.3–1.7%) and *Sphingomonadales* (1.7–2.2%) was also observed in the cathode.

At family level (Fig. 5c), *Rhodocyclaceae* (10.8–14.7%) was the most dominant in the anodic community, followed by *Anaerolineaceae* (3.0–10.6%), *Rhizobiales* (4.2–5.1%), *Planctomycetaceae* (1.4–9.7%) and *Comamonadaceae* (2.9–7.9%). In addition, various functional microorganisms (i.e., *Sphingomonadaceae* (0.3–1.2%), *Desulfuromonadaceae* (0.01–3.8%), *Desulfomicrobiaceae* (0.01–2.06%) and *Xanthomonadaceae* (0.7–3.8%), etc) were also found to be higher than other species in the anode. The highest relative abundance of *Comamonadaceae*, *Desulfuromonadaceae*, *Desulfomicrobiaceae* and *Xanthomonadaceae* was observed in the anode and cathode of T2, and the relative abundance of *Sphingomonadaceae* in T1 was higher than in other treatments. The cathodic microbial community composition of CK, T1 and T2 was similar, and was dominated by the *Planctomycetaceae* family with an abundance of 10.41% (CK), 9.28% (T1) and 9.33% (T2), respectively. In addition, *Rhodocyclaceae* (3.6–8.8%), *Hyphomicrobiaceae* (5.7–10.8%) and *Sphingomonadaceae* (1.6–2.2%) were also key cathodic families in the three types of MFC-CWs.

4. Discussion

4.1. The intensification effect of integration of MFC with CWs on nutrient removal

In this study, The NH_4^+-N removal efficiency of two types of closed-circuit MFC-CWs (T1 and T2) was slightly greater than that of open-circuit MFC-CWs (i.e., traditional CWs), indicating that the NH_4^+-N removal performance was enhanced by the integration of MFC with CWs. This phenomenon might be caused by the electron transport driven by the closed-circuit mode. The electrode can play a role as an electron acceptor for NH_4^+-N oxidation when the microenvironment is anaerobic (Srivastava et al., 2020). In addition, anaerobic NH_4^+-N oxidation

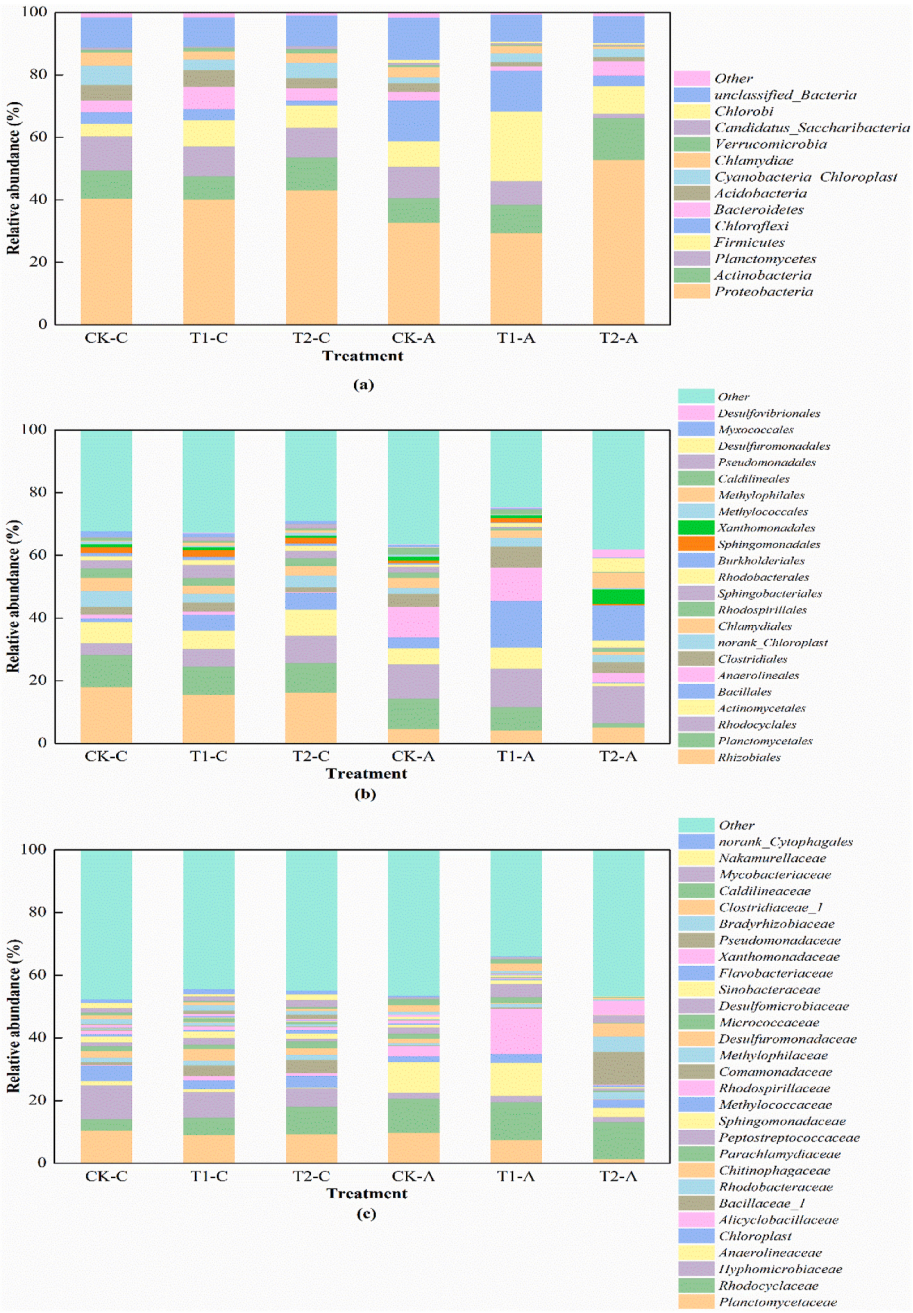

Fig. 5. Relative abundance of microbial communities of anode (CK-A, T1-A and T2-A) and cathode (CK–C, T1-C and T2-C) of different MFC-CWs (CK: open-circuit MFC-CWs; T1: closed-circuit MFC-CWs; T2: closed-circuit MFC-CWs amended with sponge iron in anode). ((a) Phylum, (b) Order, (c) Family).

induced by electron transfer also contributes to a higher NH_4^+-N removal efficiency of closed-circuit MFC-CWs (Vilajeliu-Pons et al., 2017). The NH_4^+-N removal efficiency of T2 was lower than that of T1 during the operation time, especially in the first 12 h. The difference in NH_4^+-N removal between two different reactors can be explained as: 1) sponge iron is mainly composed of abundant zero valent iron (ZVI), with a strong reduction characteristic, and the reductive atmosphere is not beneficial for ammonia oxidation; 2) Less dissolved oxygen in the MFC-CWs amended with sponge iron in the anode is a limiting factor of nitrification (Cai et al., 2018). Therefore, there was a lower chemical conversion efficiency from NH_4^+-N to NO_3^--N in T2 compared to normal MFC-CWs; 3) the anammox process in T2 may be inhibited by the microenvironment. Anammox can also play a vital role in nitrogen removal in an anaerobic environment (Wang et al., 2019b). This finding was also evidenced by the lower relative abundance of *Planctomycetes* observed in T2 compared to that of T1. Various anammox bacteria have been reported to belong to the *Planctomycetaceae* family in *Planctomycetes* phylum (Xiao et al., 2016).

Consistent with the role of O_2, NO_3^--N can also be used as an electron acceptor. The closed-circuit condition can also enhance the denitrification process by accelerating the electron transport in closed-circuit MFC-CWs. Compared to normal CWs. The highest NO_3^--N removal efficiency was observed in T2, illustrating that the addition of ZVI to the anode was beneficial for denitrification. The anaerobic environment in T2 caused by dissolved oxygen consumption benefits simultaneous heterotrophic and autotrophic denitrification or mixotrophic denitrification (Huang et al., 2015; Kumwimba et al., 2021). In addition, Fe (II) can be considered as an adjuster to regulate the bacterial biomass and improve related enzyme activity (Yang et al., 2017). In this study, the relative abundance of *Rhodocyclaceae*, *Comamonadaceae* and

Xanthomonadaceae in T2 was higher than that in other treatments irrespective of anode and cathode. Some bacteria such as *Comamonadaceae*, *Rhodocyclaceae* and *Xanthomonadaceae* are known as denitrification bacteria which can convert NO_3^--N to N_2 (Lu et al., 2015). We infer that a higher abundance of denitrifying bacteria around the electrode contributed to the better NO_3^--N removal performance of T2.

The highest TP removal efficiency among all treatments was observed in T1. Compared to CK, the average TP removal efficiency in two operation periods of T1 was increased by 41.93%, indicating that the integration of MFC into CWs can accelerate TP removal. In addition, the closed-circuit also boosted the growth of some phosphorus-accumulating bacteria in this study. Compared to open-circuit operation, a higher relative abundance of *Comamonadaceae* and *Rhodocyclaceae*, some of which are considered to be phosphorus-accumulating organisms (PAOs) (Ge et al., 2015; Kim et al., 2017), was observed under closed-circuit operation. However, the TP removal efficiency of MFC-CWs amended with sponge iron in the anode was lower than the other two treatments in contrasted with some previous study (Ge et al., 2020). The addition of sponge iron can improve TP removal due to the available Fe (II) and Fe (III) ions in the system (Xu et al., 2020). Due to abundant Fe ions in MFC-CWs system, P can be recovered as ferric phosphate and/or adsorbed onto iron hydroxide precipitates (Ge et al., 2020; Zhang et al., 2019; Zhang et al., 2020b). The difference in TP removal efficiency in this study may be due to the different selection of electrode material. The electrode material in this study consisted of GAC rather than carbon fiber felts in a previous study (Ge et al., 2020). When sponge iron was added to the anode, the specific surface area of its anode was significantly ($p < 0.05$) lower than that of the anode consisting of GAC (Table 1). In addition, more microporous structure was present in GAC anode (Table 1). The positive effect of GAC on TP adsorption may be greater than that of iron ion and their hydroxides. Thus, we infer that the decreased adsorption capacity of T2 resulted in the unsatisfactory TP removal efficiency.

4.2. The intensification effect of MFC-CWs on MC-LR removal

Various chemical reactions that are occurring due to the existence of electrodes may accelerate the degradation of bio-refractory compounds. In this study, MC-LR removal efficiency of T1 was significantly ($p < 0.05$) higher than that of the control. The effluent MC-LR concentration of T1 was reduced to below the safety guideline (1 μg/L) within 2 d, demonstrating that a closed-circuit connection could enhance the MC-LR removal efficiency. Compared with MCs removal efficiency (Table 3) obtained in other normal CWs, more MC-LR can be eliminated in T1 with a shorter HRT (Wang et al., 2018; Bavithra et al., 2020; Cheng et al., 2021). For closed-circuit MFC-CWs, the facilitation of microbial electron transfer may improve the utilization of bioavailable organic matter (Ge et al., 2020). Biodegradation of bio-refractory compounds (e.g., PPCPs, azo dyes and antibiotics) mainly occurs in the anode layer which can provide a more favorable temporary electron pathway under closed-circuit conditions compared with using oxygen as the electron acceptor under open-circuit conditions (Yuan et al., 2011; Li et al., 2018). In addition, there was improved electron adsorption ability under closed circuit conditions, which may have enhanced MC-LR trapping ability of the system (Song et al., 2018). Moreover, the presence of a closed-circuit connection could improve the microbial activity. The complete degradation of MCs gradually depended on indigenous microcystin-degrading bacteria in the natural environment (Dziga et al., 2013). Many microcystin-degrading bacteria were recognized from the family *Sphingomonadaceae*, whose microcystins degradation process is regulated by the specific enzymes coded by a series of *mlr* genes (Lezcano et al., 2017; Li et al., 2017). According to microbial community analysis, the relative abundance of *Sphingomonadaceae* in the anode and cathode of T1 was 1.53 and 1.16 times higher than that of CK. The highest abundance of degrading bacteria also contributed to the highest MC-LR removal efficiency of T1.

Table 3
Summary of MCs removal performance in different CWs.

No.	CWs type	HRT	MCs type	Influent MCs concentration	Removal efficiency	References
1	MFC-CWs	2 days	MC-LR	15 μg/L	97.19%	This study
2	Normal CWs	5 days	MC-LR	14.41 μg/L	79.55%–93.61%	Cheng et al. (2021)
3	Normal CWs	7 days	MC-LR	0.21–4 μg/L	>99%	Bavithra et al. (2020)
4	Normal CWs	3 days	MC-LR	16.7 μg/L	>90%	Wang et al. (2018)

The MC-LR removal efficiency of T2 was the lowest in this study. After 2 days treatment, the effluent MC-LR concentration was still higher than the safety guideline of 1.0 μg/L in drinking water, indicating that the application of sponge iron cannot enhance MC-LR removal efficiency, although several previous studies proposed that the addition of ZVI into the anode was conducive to bio-refractory compounds degradation in the MFC-CWs (Zhang et al., 2011; Wang et al., 2019a). The main reasons are as follows: 1) due to the addition of sponge iron, the surface area and total pore volume of the anode decreased compared to that of CK and T1 (Table 1). This result illustrated that the MC-LR adsorption capacity of the system decreased compared to that of CK and T1; 2) the lower MC-LR removal efficiency in T2 may also be attributed to the higher external resistance. As presented above in the Results section, the internal resistance of T2 was 217.18 Ω, which was much lower than the external resistance (1000 Ω), while the internal resistance of T1 (1138.8 Ω) was closer to the external resistance (1000 Ω). As clarified in previous study, the highest removal efficiency usually occurred when the external resistance was close to the internal resistance in MFC-CWs (Fernando et al., 2014; Wen et al., 2021a), mainly due to the decreased consumption of metabolites caused by the reduction of respiration rate and electron transfer activity under higher external resistance (Aelterman et al., 2008; Gul et al., 2021); 3) the relative abundance of *Sphingomonadaceae* of T2 was lower than that of CK and T1, especially in the anode layer. To summaries, the addition of sponge iron into anode was not conducive to the growth and reproduction of MCs degrading bacteria.

4.3. Bioelectricity generation performance of MFC-CWs enhanced by sponge iron

Voltage output, current density and power density of T2 were significantly ($p < 0.05$) improved compared to that of T1. T2 also showed significantly ($p < 0.05$) lower internal resistances than T1. The bioelectricity generation performance of T2 was also superior to that obtained by Srivastava et al. (2020) and Liu et al. (2020) for MFC-CWs planted with common sedges (*Carexbreviculmis*) (27.2–42.0 mV) and yellow iris (*Iris pseudacorus*) (132 ± 42 mV). This observation can be explained as follows: 1) ZVI addition into the anode can reduce the oxidation reduction potential (ORP) of the microenvironment of T2 (Liu and Wang, 2019). ZVI can also facilitate electron transfer and enzyme activity, thus strengthening the bioelectricity generation performance of MFC-CWs (Harada et al., 2016). 2) In this study, the relative abundance of EAB enhanced by sponge iron addition may also contribute to improved bioelectricity generation performance (Wang et al., 2019b). As presented in Fig. 5a, *Proteobacteria* and *Firmicutes* were widely distributed in the anode of two types of MFC-CWs, and most EAB belongs to these above phyla (Lu et al., 2015). Therefore, the higher relative abundance of the above two phyla in the anode of T2 can enhance its potential for electrogenic activity (Li et al., 2018). Microbial community analysis indicated that, certain families of *Proteobacteria*, such as *Desulfuromonadaceae* and *Desulfomicrobiaceae* were the two dominant EAB; both can directly or indirectly transfer electrons generated in the degradation process of organic matter to the external circuit generating

current (Miyahara et al., 2016; Hamdan et al., 2016). Although the improved bioelectricity generation performance was presented in T2, the acceptable TP and MC-LR removal performance was not observed due to the selection of external resistance and electrode materials. Therefore, more systematic research is recommended to focus on optimizing the design and operation (e.g., reactor configuration, electrode material and operating condition, etc.) of MFC-CWs to achieve an increase in both pollutant removal and bioelectricity generation.

5. Conclusion

In this study, the enhancing of nutrient and MC-LR removal by MFC-CWs was comprehensively evaluated. The main conclusions are as follows: 1) the closed-circuit MFC-CWs enhanced the nutrient and MC-LR removal efficiency compared to open-circuit MFC-CWs; 2) although the addition of sponge iron into anode layer can improve the bioelectricity generation performance, the TP and MC-LR removal efficiency was lower than that of normal MFC-CWs due to imperfect operational conditions and electrode materials; 3) the addition of sponge iron into the anode reduced microbial richness and diversity of the microbial community compared to traditional MFC-CWs. The relative abundance of EAB increased, while the relative abundance of microcystin-degrading bacteria decreased. The above results demonstrate that integrating MFC into CWs can be viewed as an alternative intensification strategy for using CWs to target eutrophication and MCs pollution control. In order to achieve more pollutant removal and energy recovery, future research should concentrate on optimizing the design and operation of MFC-CWs.

Credit Author Statement

Rui Cheng: Methodology, Investigation, Writing – original draft. **Hui Zhu:** Resources, Writing – review & editing, Project administration, Supervision, Funding acquisition. **Jingfu Wang:** Resources, Project administration, Funding acquisition. **Shengnan Hou:** Investigation, Writing – review & editing. **Brian Shutes:** Writing – review & editing. **Baixing Yan:** Resources.

Declaration of competing interest

The authors declare that they have no known competing financial interests or personal relationships that could have appeared to influence the work reported in this paper.

Acknowledgments

This work was supported by the CAS Interdisciplinary Innovation Team Project (No. JCTD-2020-14), and the Youth Innovation Promotion Association, CAS (No. 2017274).

Appendix A. Supplementary data

Supplementary data to this article can be found online at https://doi.org/10.1016/j.jenvman.2022.114669.

References

Aelterman, P., Versichele, M., Marzorati, M., Boon, N., Verstraete, W., 2008. Loading rate and external resistance control the electricity generation of microbial fuel cells with different three-dimensional anodes. Bioresour. Technol. 99 (18), 8895–8902.

Bavithra, G., Azevedo, J., Oliveira, F., Morais, J., Pinto, E., Ferreira, I., Vasconcelos, V., Campos, A., Almeida, C.M.R., 2020. Assessment of constructed wetlands' potential for the removal of cyanobacteria and microcystins (MC-LR). Water 12, 10.

Cai, L., Zhang, H., Feng, Y., Wang, Y., Yu, M., 2018. Sludge decrement and electricity generation of sludge microbial fuel cell enhanced by zero valent iron. J. Clean. Prod. 174, 35–41.

Chen, X., Zhu, H., Banuelos, G., Shutes, B., Yan, B., Cheng, R., 2020. Biochar reduces nitrous oxide but increases methane emissions in batch wetland mesocosms. Chem. Eng. J. 392, 124842.

Cheng, R., Zhu, H., Shutes, B., Yan, B., 2021. Treatment of microcystin (MC-LR) and nutrients in eutrophic water by constructed wetlands: performance and microbial community. Chemosphere 263, 128139. https://doi.org/10.1016/j.chemosphere.

Conley, D.J., Paerl, H.W., Howarth, R.W., Boesch, D.F., Seitzinger, S.P., Havens, K.E., Lancelot, C., Likens, G.E., 2009. Controlling eutrophication: nitrogen and phosphorus. Science 323 (5917), 1014–1015.

Dixit, F., Barbeau, B., Mohseni, M., 2019. Removal of Microcystin-LR from spiked natural and synthetic waters by anion exchange. Sci. Total Environ. 655, 571–580.

Doherty, L., Zhao, Y., Zhao, X., Hu, Y., Hao, X., Xu, L., Liu, R., 2015. A review of a recently emerged technology: constructed wetland–microbial fuel cells. Water Res. 85, 38–45.

Dziga, D., Wasylewski, M., Wladyka, B., Nybom, S., Meriluoto, J., 2013. Microbial degradation of microcystins. Chem. Res. Toxicol. 26 (6), 841–852.

Fernando, E., Keshavarz, T., Kyazze, G., 2014. External resistance as a potential tool for influencing azo dye reductive decolourisation kinetics in microbial fuel cells. Int. Biodeterior. Biodegrad. 89, 7–14.

Ge, H., Batstone, D.J., Keller, J., 2015. Biological phosphorus removal from abattoir wastewater at very short sludge ages mediated by novel PAO clade *Comamonadaceae*. Water Res. 69, 173–182.

Ge, X., Cao, X., Song, X., Wang, Y., Si, Z., Zhao, Y., Wang, W., Tesfahunegn, A.A., 2020. Bioenergy generation and simultaneous nitrate and phosphorus removal in a pyrite-based constructed wetland-microbial fuel cell. Bioresour. Technol. 296, 122350. https://doi.org/10.1016/j.biortech.

Gul, H., Raza, W., Lee, J., Azam, M., Ashraf, M., Kim, K.H., 2021. Progress in microbial fuel cell technology for wastewater treatment and energy harvesting. Chemosphere. https://doi.org/10.1016/j.chemosphere, 130828.

Hamdan, H.Z., Salam, D.A., Hari, A.R., Semerjian, L., Saikaly, P., 2016. Assessment of the performance of SMFCs in the bioremediation of PAHs in contaminated marine sediments under different redox conditions and analysis of the associated microbial communities. Sci. Total Environ. 1453.

Harada, T., Yatagai, T., Kawase, Y., 2016. Hydroxyl radical generation linked with iron dissolution and dissolved oxygen consumption in zero-valent iron wastewater treatment process. Chem. Eng. J. 303, 611–620.

Huang, X., Liu, C., Li, K., Su, J., Zhu, G., Liu, L., 2015. Performance of vertical up-flow constructed wetlands on swine wastewater containing tetracyclines and tet genes. Water Res. 70, 109–117.

Kim, E., Shin, S.G., Jannat, M.A.H., Tongco, J.V., Hwang, S., 2017. Use of food waste-recycling wastewater as an alternative carbon source for denitrification process: a full-scale study. Bioresour. Technol. 245, 1016. https://doi.org/10.1016/j.biortech.

Kim, M., Kim, D., Kim, J., Hong, S., Shin, K., 2021. Distribution of microcystins in environmental multimedia and their bioaccumulation characteristics in marine benthic organisms in the Geum River Estuary, South Korea. Sci. Total Environ. 757, 143815.

Kumwimba, M.N., Batool, A., Li, X., 2021. How to enhance the purification performance of traditional floating treatment wetlands (FTWs) at low temperatures: strengthening strategies. Sci. Total Environ. 766, 142608. https://doi.org/10.1016/j.scitotenv.

Lezcano, M.Á., Velázquez, D., Quesada, A., El-Shehawy, R., 2017. Diversity and temporal shifts of the bacterial community associated with a toxic cyanobacterial bloom: an interplay between microcystin producers and degraders. Water Res. 52–61.

Li, H., Zhang, S., Yang, X., Yang, Y.L., Xu, H., Li, X., Song, H., 2018. Enhanced degradation of bisphenol A and ibuprofen by an up-flow microbial fuel cell-coupled constructed wetland and analysis of bacterial community structure. Chemosphere 217, 599–608.

Li, J., Li, R., Li, J., 2017. Current research scenario for microcystins biodegradation–a review on fundamental knowledge, application prospects and challenges. Sci. Total Environ. 595, 615–632.

Li, X., Huang, Y., Liu, H.W., Wu, C., Bi, W., Yuan, Y., Liu, X., 2018. Simultaneous Fe (III) reduction and ammonia oxidation process in Anammox sludge. J. Environ. Sci. 64, 42–50.

Liang, Y., Zhu, H., Banuelos, G., Shutes, B., Yan, B., Cheng, X., 2018. Removal of sulfamethoxazole from salt-laden wastewater in constructed wetlands affected by plant species, salinity levels and co-existing contaminants. Chem. Eng. J. 341, 462–470.

Lin, H., Liu, W., Zeng, H., Pu, C., Zhang, R., Qiu, Z., 2016. Determination of environmental exposure to microcystin and aflatoxin as a risk for renal function based on 5493 rural people in southwest China. Environ. Sci. Technol. 50 (10), 5346–5356.

Liu, X., Liang, C., Liu, X., Lu, S., Xi, B., 2020. Intensified pharmaceutical and personal care products removal in an electrolysis-integrated tidal flow constructed wetland. Chem. Eng. J. 394, 124860.

Liu, Y., Wang, J., 2019. Reduction of nitrate by zero valent iron (ZVI)-based materials: a review. Sci. Total Environ. 671, 388–403.

Lu, L., Xing, D., Ren, Z., 2015. Microbial community structure accompanied with electricity production in a constructed wetland plant microbial fuel cell. Bioresour. Technol. 195, 115–121.

Lutterbeck, C.A., Machado, È.L., Sanchez-Barrios, A., Silveira, E.O., Layton, D., Rieger, A., Lobo, E.A., 2020. Toxicity evaluation of hospital laundry wastewaters treated by microbial fuel cells and constructed wetlands. Sci. Total Environ. 729, 138816.

Machado, J., Campos, A., Vasconcelos, V., Freitas, M., 2017. Effects of microcystin-LR and cylindrospermopsin on plant-soil systems: a review of their relevance for agricultural plant quality and public health. Environ. Res. 153, 191–204.

Miyahara, M., Sakamoto, A., Kouzuma, A., Watanabe, K., 2016. Poly iron sulfate flocculant as an effective additive for improving the performance of microbial fuel cells. Bioresour. Technol. 221, 331–335.
Morón-López, J., Nieto-Reyes, L., Senán-Salinas, J., Molina, S., El-Shehawy, R., 2019. Recycled desalination membranes as a support material for biofilm development: a new approach for microcystin removal during water treatment. Sci. Total Environ. 647, 785–793.
Pham, T.L., Utsumi, M., 2018. An overview of the accumulation of microcystins in aquatic ecosystems. J. Environ. Manag. 213, 520–529.
Prathiba, S., Kumar, P.S., Vo, D.V.N., 2022. Recent advancements in microbial fuel cells: a review on its electron transfer mechanisms, microbial community, types of substrates and design for bio-electrochemical treatment. Chemosphere 286, 131856. https://doi.org/10.1016/j.chemosphere.
Shi, K., Zhang, Y., Xu, H., Zhu, G., Qin, B., Huang, C., Liu, X., Zhou, Y., Lv, H., 2015. Long-term satellite observations of microcystin concentrations in Lake Taihu during cyanobacterial bloom periods. Environ. Sci. Technol. 49 (11), 6448–6456.
Song, H., Li, H., Zhang, S., Yang, Y., Zhang, L., Xu, H., Yang, X., 2018. Fate of sulfadiazine and its corresponding resistance genes in up-flow microbial fuel cell coupled constructed wetlands: effects of circuit operation mode and hydraulic retention time. Chem. Eng. J. 350, 920–929.
Srivastava, P., Yadav, A.K., Garaniya, V., Lewis, T., Abbassi, R., Khan, S.J., 2020. Electrode dependent anaerobic ammonium oxidation in microbial fuel cell integrated hybrid constructed wetlands: a new process. Sci. Total Environ. 698, 134248.
Tsao, S., Wei, D.J., Chang, Y.T., Lee, J.F., 2017. Aerobic biodegradation of microcystin-LR by an indigenous bacterial mixed culture isolated in Taiwan. Int. Biodeterior. Biodegrad. 124, 101–108.
Vilajeliu-Pons, A., Puig, S., Salcedo-Dávila, I., Balaguer, M.D., Colprim, J., 2017. Long-term assessment of six-stacked scaled-up MFCs treating swine manure with different electrode materials. Environ. Sci-Wat. Res. 3 (5), 947–959.
Wang, H., Xu, C., Liu, Y., Jeppesen, E., Svenning, J.C., Wu, J., Zhang, W., Zhou, T., Wang, P., Nangombe, S., Ma, J., Duan, H., Fang, J., Xie, P., 2021. From unusual suspect to serial killer: cyanotoxins boosted by climate change may jeopardize megafauna. Innovation 2 (2), 100092.
Wang, J., Song, X., Li, Q., Bai, H., Zhu, C., Weng, B., Yan, D., Bai, J., 2019a. Bioenergy generation and degradation pathway of phenanthrene and anthracene in a constructed wetland-microbial fuel cell with an anode amended with nZVI. Water Res. 150, 340–348.
Wang, M., Shi, W., Chen, Q., Zhang, J., Yi, Q., Hu, L., 2018. Effects of nutrient temporal variations on toxic genotype and microcystin concentration in two eutrophic lakes. Ecotoxicol. Environ. Saf. 166, 192–199.
Wang, S., Wang, W., Zhao, S., Wang, X., Hefting, M.M., Schwark, L., Zhu, G., 2019b. Anammox and denitrification separately dominate microbial N-loss in water saturated and unsaturated soils horizons of riparian zones. Water Res. 162, 139–150.
Wang, W., Zhang, Y., Li, M., Wei, X., Wang, Y., Liu, L., Wang, H., Shen, S., 2020. Operation mechanism of constructed wetland-microbial fuel cells for wastewater treatment and electricity generation: a review. Bioresour. Technol. 123808 https://doi.org/10.1016/j.biortech.
Wen, H., Zhu, H., Xu, Y., Yan, B., Shutes, B., Bañuelos, G., Wang, X., 2021a. Removal of sulfamethoxazole and tetracycline in constructed wetlands integrated with microbial fuel cells influenced by influent and operational conditions. Environ. Pollut. 272, 115988. https://doi.org/10.1016/j.envpol.
Wen, H., Zhu, H., Yan, B., Shutes, B., Yu, X., Cheng, R., Chen, X., Wang, X., 2021b. Constructed wetlands integrated with microbial fuel cells for COD and nitrogen removal affected by plant and circuit operation mode. Environ. Sci. Pollut. Res. 28 (3), 3008–3018.
Wen, H., Zhu, H., Yan, B., Xu, Y., Shutes, B., 2020. Treatment of typical antibiotics in constructed wetlands integrated with microbial fuel cells: roles of plant and circuit operation mode. Chemosphere 250, 126252. https://doi.org/10.1016/j.chemosphere.
World Health Organization (WHO), 2017. Guidelines for drinking-water quality. In: Incorporating the 1st Addendum, fourth ed. World Health Organization, Geneva.
Xiao, K., Zhou, L., He, B., Qian, L., Wan, S., Qu, L., 2016. Nitrogen and phosphorus removal using fluidized-carriers in a full-scale A^2O biofilm system. Biochem. Eng. J. 115, 47–55.
Xu, F., Ouyang, D.L., Rene, E.R., Ng, H.Y., Guo, L., Zhu, J., Zhou, L., Yuan, Q., Miao, M., Wang, Q., Kong, Q., 2019. Electricity production enhancement in a constructed wetland-microbial fuel cell system for treating saline wastewater. Bioresour. Technol. 288, 121462.
Xu, F., Zhu, Y., Wang, Y., Chen, H., Zhang, Y., Hao, D., Qi, X., Du, Y., Wang, B., Wang, Q., Zhao, C., Kong, Q., 2020. Coupling iron pretreatment with a constructed wetland-microbial fuel cell to improve wastewater purification and bioelectricity generation. J. Clean. Prod. 276, 123301. https://doi.org/10.1016/j.jclepro.
Yang, B., Xu, H., Wang, J., Song, X., Wang, Y., Li, F., Tian, Q., Ma, C., Wang, D., Bai, J., Sand, W., 2017. Bacterial and archaeal community distribution and stabilization of anaerobic sludge in a strengthen circulation anaerobic (SCA) reactor for municipal wastewater treatment. Bioresour. Technol. 750 https://doi.org/10.1016/j.biortech.
Yu, X., Zhu, H., Yan, B., Xu, Y., Bañuelos, G., Shutes, B., Wen, H., Cheng, R., 2019. Removal of chlorpyrifos and its hydrolytic metabolite 3, 5, 6-trichloro-2-pyridinol in constructed wetland mesocosms under soda saline-alkaline conditions: effectiveness and influencing factors. J. Hazard Mater. 373, 67–74.
Yuan, Y., Chen, Q., Zhou, S., Zhuang, L., Hu, P., 2011. Bioelectricity generation and microcystins removal in a blue-green algae powered microbial fuel cell. J. Hazard Mater. 187 (1–3), 591–595.
Zhang, J., Djellabi, R., Zhao, S., Qiao, M., Jiang, F., Yan, M., Zhao, X., 2020. Recovery of phosphorus and metallic nickel along with HCl production from electroless nickel plating effluents: the key role of three-compartment photoelectrocatalytic cell system. J. Hazard Mater. 394, 122559. https://doi.org/10.1016/j.jhazmat.
Zhang, J., Zhang, Y., Quan, X., Liu, Y., An, X., Chen, S., Zhao, H., 2011. Bioaugmentation and functional partitioning in a zero valent iron-anaerobic reactor for sulfate-containing wastewater treatment. Chem. Eng. J. 174 (1), 159–165.
Zhang, J., Zhao, X., Wang, Y., Djellabi, R., 2019. Recovery of phosphorus from hypophosphite-laden wastewater: a single-compartment photoelectrocatalytic cell system integrating oxidation and precipitation. Environ. Sci. Technol. 54 (2), 1204–1213.
Zhu, G., Wang, S., Feng, X., Fan, G., Jetten, M.S., Yin, C., 2011. Anammox bacterial abundance, biodiversity and activity in a constructed wetland. Environ. Sci. Technol. 45 (23), 9951–9958.